Sustainable Energy & Fuels

ROYAL SOCIETY OF CHEMISTRY

PAPER

View Article Online
View Journal | View Issue

Cite this: *Sustainable Energy Fuels*, 2023, 7, 752

P-containing coated carbons from phosphonium ionic liquids as catalyst supports for fuel cell applications†‡

Angelo A. Severin, *[a] Daniel Rauber, [ab] Stavroula Pachoula,[a] Frederik Philippi, §[a] Ivan Radev,[c] Anne Holtsch,[d] Frank Müller,[d] Manfred Baumgärtner,[e] Rolf Hempelmann [b] and Christopher W. M. Kay*[af]

Research on heteroatom doping of carbon materials for advanced electrochemical devices such as fuel cells became prominent over the last decade to improve longevity and performance, with phosphorus-containing, nitrogen-free carbons seldom investigated. Here, we show that precursors coated with P-containing carbon, as supports for noble metal catalysts, enhance the performance and durability of cathodes in fuel cell operation. Simple wet coating of a series of carbon substrates with ionic liquids and subsequent pyrolysis at 400 °C produced carbon materials with homogeneously distributed phosphorus atoms. This process is applicable to a variety of different carbons, yielding P-content up to 3.0 wt% with PO_3^- and PO_4^- like species as confirmed by XPS-measurements. Fuel cell test systems revealed not only superior performance but also enhanced durability. The results show that small amounts of surface phosphorus on carbon supports have a positive impact on key characteristics including reduced ohmic and cathode transfer resistances. In addition, durability and ORR activity were improved with neither the morphology nor the geometry being significantly affected. We explain our observation regarding different modifications of the structure and surface of carbon materials as being due to new and favourable active sites provided by the bond length, atomic radius, and electronegativity of the introduced phosphorus species. The novelty of this approach is the formation of PO_4^- like species from ionic liquids at relatively low pyrolysis temperatures, which promotes improved ORR activity. Ionic liquids can serve as precursors for heteroatom-containing carbon-based materials with improved properties, opening a new avenue for the fabrication of devices in which carbon-based materials are utilized.

Received 26th September 2022
Accepted 5th December 2022

DOI: 10.1039/d2se01332k

rsc.li/sustainable-energy

1. Introduction

Carbon materials are widely used in different energy conversion technologies such as fuel cells, batteries or supercapacitors.[1] The utilization of carbon materials containing heteroatoms (also often referred to as heteroatom-doped carbons, although the content of heteroatoms might be quite high) such as nitrogen, sulphur, boron or phosphorus aids in improving various characteristics of the said technologies. Heteroatom-containing carbons provide a series of beneficial features in comparison to their non-doped counterparts due to their different numbers of valence electrons, atomic radii, binding energies, and electronegativity (EN). This results in changes of the carbon matrix where open edges (induced by defects) or the doped groups themselves provide active sites where the desired reaction takes place.[2] For example, nitrogen can form five different configurations in a graphitic system: pyrollic, graphitic, pyridinic or as pyridinium and pyridine oxide.[3,4] Nitrogen-containing carbons are known to have a positive impact on the oxygen reduction reaction (ORR) of noble metal catalysts (*i.e.*, stability and durability) and may even be suitable as standalone metal-free electro-catalysts in some cases.[5–7] While nitrogen doping and the synthesis of N-containing carbons have been extensively studied, research on the utilization of the doping with the higher homologue, phosphorus, is

[a]*Department of Chemistry, Saarland University, Campus B2 2, 66123 Saarbrücken, Germany. E-mail: angelo.stephan@uni-saarland.de; Tel: +49 681 302 64310*

[b]*Transfercenter Sustainable Electrochemistry, Saarland University, Am Markt, Zeile 3, 66125 Saarbrücken, Germany*

[c]*The Hydrogen and Fuel Cell Center ZBT GmbH, Carl-Benz-Straße 201, 47057 Duisburg, Germany*

[d]*Experimental Physics and Center for Biophysics, Saarland University, Campus E2 9, 66123 Saarbrücken, Germany*

[e]*Research Institute for Precious Metals and Metal Chemistry, Katharinenstraße 17, 73525 Schwäbisch Gmünd, Germany*

[f]*London Centre for Nanotechnology, University College London, Gordon Street 17-19, London WC1H 0AH, UK. E-mail: c.kay@ucl.ac.uk; Tel: +44 (0)207 679 7312*

† Dedicated to our colleague PD Dr Harald Natter (1966–2020) who initiated this work and passed away too early.

‡ Electronic supplementary information (ESI) available. See DOI: https://doi.org/10.1039/d2se01332k

§ Current address: Department of Chemistry & Life Science, Yokohama National University, 79-5 Tokiwadai, Hodogaya-ku, Yokohama, 240-8501 Japan.

comparatively rare. Therefore, studies on synthesis and characteristics of P-containing carbon (PCC) materials might help to improve the performance and durability of different technologies where carbon materials are already utilized.

2. Theory

Phosphorus is a promising heteroatom dopant to alter carbon properties in beneficial ways for utilization in various fields of technology. First of all, P creates hydrophilic acidic surfaces when incorporated into graphitic structures.[8] This surface modification arises from residual phosphate ($O–PO_3$) and phosphite ($O–PO_2$) species which induce high water affinity. Additionally, treating carbons with P-containing precursors increases acidic properties in the respective carbon materials. Several studies with different analytical methods confirmed the formation of acidic groups possessing proton affinity where the quantity of acidic groups is mostly linear to the P-content.[9–11] Furthermore, an increase in proton conductivity can be induced by acidic groups. Another advantage of PCCs is that the P-containing surface groups enhance oxidation resistance of carbon supports by acting as physical barriers.[12] This avoids the burn-off (degradation) of the carbon support in reactions involving oxygen, for example during the catalytic oxidation of toluene to benzoic acid. These characteristics of PCC noble metal catalyst supports were also reported by other groups.[13,14] A further advantage of P-containing carbons is their enhanced electrical conductivity compared to phosphorus-free materials. With increasing P-content in both tetrahedral-amorphous (ta) and diamond-like (dl) carbons, the electrical conductivity of the resulting PCC materials could be increased.[15–17] This phenomenon was explained by substitution of phosphorus into the carbon structure and increasing graphitization, though no experimental evidence was provided by the authors. Nonetheless, other investigations proved the graphitizing properties of phosphorus at high temperatures (up to 3000 °C) when introduced in phenol-formaldehyde-based carbon fibers.[18] The displayed advantages of phosphorus doping, such as the formation of hydrophilic species and acidic surfaces, and enhanced durability and electronic conductivity promote the use of PCCs in various technologies where the utilization of carbon substrates already takes place.

The coating and pyrolysis method used in this work allows for a large variety of options for electrochemical applications because theoretically any carbon substrate may be suitable for the presented method of generating P-coated carbon materials. The ionic liquids were used as a precursor for the formation of P-containing carbon on the surface of commercial carbon substrates. The heteroatom-doping is not limited to phosphorus alone. Co-doping with nitrogen or other elements is also possible by adjusting the used ionic liquid. In this work, the resulting P-coated materials were examined by X-ray photoelectron spectroscopy (XPS), and the pressure-dependent conductivity of the powders was measured. The suitability of P-coated carbons as catalyst supports for fuel cell utilization was investigated by half and full cell measurements. The results showed superior fuel cell characteristics for P-coated carbon catalyst support materials including increased electrical conductivity, and improved activity, durability, and stability.

3. Synthesis

Details of all experimental methods and parameters, measured data points and fitting procedures as well as NMR spectra and reaction conditions are given in the ESI.‡

Phosphorus-coated carbon materials were synthesized by the wet impregnation method followed by pyrolysis in a tube furnace. For the wet impregnation method, 1 mmol of ionic liquid was dissolved in 25 mL of isopropyl alcohol and added to 0.5 g of pristine carbon black or carbon nanotubes. The mixture was slowly stirred and heated at 80 °C to evaporate isopropyl alcohol. The coated carbons were then heated at 400 °C under a N_2 atmosphere in a tube furnace. These coating and pyrolysis conditions turned out to be the optimum among many various tested settings. For example, other conditions included solvents like ethanol or acetonitrile, higher/lower ratios of ionic liquid to the carbon substrate and heat treatment at 800 °C and 1000 °C. Detailed information regarding the optimization process will be given below.

Platinum deposition for half-cell measurements was performed by chemical reduction using a modified literature method.[19] For a typical deposition, 50 mg of carbon material was mixed with 53 mg of hexachloroplatinic acid hydrate (40 wt% platinum content) and 9 mL of water in a flask. The mixture was placed in an ultrasonic bath for 30 min. Then, 36 mL of ethylene glycol was added to the mixture. The chemical reduction was performed at 120 °C bath temperature for 24 h under reflux. Purification was achieved by washing with ethanol and centrifugation. The platinum-decorated carbon was dried at 80 °C.

4. Results and discussion

The physicochemical characterization of the synthesized ionic liquids is described in the ESI.‡ We analysed the thermal properties *via* differential scanning calorimetry (DSC) and thermo-gravimetric analysis (TGA), the dynamic viscosity *via* a rheometer, specific and molar conductivity by means of impedance spectroscopy and self-diffusion coefficients *via* PFGSTE NMR. Furthermore, the correlation between the transport properties was estimated using Walden and Nernst–Einstein relations. The molecular structures, abbreviations and full descriptions of the ions used in the ionic liquids are provided in the ESI in Fig. S1.‡ The main article will focus on PCC materials and their characterization. The first approaches and following optimization steps leading to the final synthesis procedure alongside the parameters are described in the ESI.‡ We choose to focus our investigations on Vulcan®-XC72R carbon black (referred to as CB) and multi-walled carbon nanotubes (referred to as CNT) because these two materials hold the most promising potential for fuel cell applications.

The fuel cell tests are presented in the ESI (see Fig. S9–S11‡) and were conducted using a phosphorus-coated carbon black material. Carbon black was used as the substrate and the ionic

liquid [P_{4442}][DEP] as the phosphorus source. For this material, dichloromethane was used as organic solvent and pyrolysis was conducted at 800 °C. The phosphorus content in the corresponding sample was 0.10 wt% and the resulting increase in powder conductivity was 8.1% (4.1 S cm^{-1}). The material is referred to as P-CB in the figures and paragraphs related to fuel cell testing. Three diverse types of settings were used for fuel cell testing: without plasma treatment, with plasma treatment by FEM (denoted as PT-FEM) and with plasma treatment by Plasmatreat GmbH (denoted as PT-PTR). Plasma treatment prior to catalyst deposition was proven to have beneficial effects on the cathode performance.[20] Investigations showed that plasma partially destroys the PTFE coating in the membrane electrode assembly, ensuring a thin hydrophilic layer which enables proper Pt electrodeposition at the catalyst layer and preserves the humidity of the membrane. Since plasma treatment occurs on the material surface and is easily controllable, the rest of the microporous layers remains hydrophobic. Thus, the removal of excess water during fuel cell operation could still be promoted reducing flooding of the catalyst layer. The coexistence of both hydrophilic and hydrophobic moieties through plasma treatment boosts fuel cell performance and is therefore desirable. Full cell measurements were carried out for cathodes consisting of a simple gas diffusion system (GDS) and those coated with pure CB and P-CB, respectively. As stated in the ESI,‡ a platinum–phosphorus alloy (denoted as PtP) with a phosphorus content of 1 wt% was used as an ORR catalyst. For all displayed results, the anode and the cathode gas stoichiometry coefficient λ was 3.

The results indicate that the cathode charge transfer resistance is the major factor in terms of MEA-performance. The positive effect of phosphorus coating can be seen in the resistance values of the *U*|*j*-curves. For all three types of measurements, gas diffusion systems (GDSs) coated with P-CB possessed the most favourable *U*|*j*-curves and therefore the highest cathode performance and durability. This suggests that phosphorus groups provided by P-CB function as carriers for a proton conduction mechanism from the anode to cathode. Thus, acidic phosphorus groups can improve proton conductivity, benefiting overall fuel cell performance. In addition, phosphorus coating increases not only the performance but also the durability of cathodes which can be seen when comparing the results of aged cathodes. This behaviour confirms the beneficial influence of phosphorus for carbon support materials. In terms of overall resistances, the P-CB samples showed especially lower cathode charge transfer and oxygen diffusion resistances due to improved electrical conductivity, lower hydrophobicity and therefore a higher ECSA and a lower R_c of the electrodeposited PtP catalysts. In the whole fuel cell testing, the gas diffusion systems coated with P-CB and prepared with plasma treatment from Plasmatreat GmbH are the most favourable and promising samples toward the ORR of all investigated combinations of the investigated material.

Lu *et al.*[21] investigated the incorporation of phosphorus in a platinum layer near the surface, which may be similar to the used phosphorus-doped platinum catalyst. The authors found that both current and power density could be significantly boosted by P incorporation in full cell measurements. The authors suggested that structural advantages such as concave Pt-defects from inhomogeneous bond lengths from Pt–P lead to lattice distortion and micro strains, which boosts ORR activity. This stems from a reduction in the energy barrier between adsorbed water and adsorbed oxygen. Convex Pt-defects seem to be inactive for ORR activity. In a similar fashion, PCCs with their structural and electronic advantages may have a boosting effect on the PtP-catalyst used for the fuel cell investigations.

For the sample description the following format was used: "carbon material/ionic liquid" for the formation of PCCs. The most promising combinations of carbon substrates and ionic liquids were determined by preliminary half-cell-measurements (see Fig. 1). Half-cell measurements were conducted using CV and RDE techniques in a three-electrode arrangement. The charging profiles and electrochemical active surface areas of platinum-deposited PCC were obtained from CV measurements in N_2-saturated electrolyte. Mass specific activity towards the ORR was determined with an RDE setup measuring oxygen reduction in O_2-saturated electrolyte. The mass specific activity towards the ORR is a good indicator to identify combinations of carbon substrates and ionic liquids suitable for subsequent full-cell measurements. To determine the general effect of the coating procedure and temperature treatment a blank coating was performed. For this blank sample, the respective carbon material was subjected to the general coating procedure but without addition of the ionic liquid, which reveals the effects the thermal treatment itself might have on the ORR characteristics of the carbon materials.

Fig. 1a and b show the resulting activities and Table S1‡ the corresponding platinum loadings of the prepared catalysts. A clear trend can be observed. Catalysts with P-coated carbons increase the mass specific activity compared to catalysts with the pure and untreated material. In addition to the increase in mass specific activity, every catalyst with phosphorus-coated carbon black shows superior ORR activity compared to the HISPEC® 4000 platinum standard (nominally 40 wt% Pt/C, Johnson Matthey). For catalysts with P-coated carbon nanotubes, the increase of mass specific activities is not as remarkable as for P-coated carbon black, but nonetheless significant. Wu *et al.*[22] achieved similar results, where the half-wave potential in LSV curves could be significantly reduced for P-doped carbon hollow spheres. This increase in the ORR activity of catalysts with P-coated carbons from ionic liquids is promising for fuel cell applications. According to the RDE measurements, the coating procedure seems to have remarkable impact on the ORR activity of catalysts for both carbon substrates. For carbon black catalysts, the effect of the coating procedure towards mass specific activity is quite strong. The activity of catalysts with blank CB surpasses not only the untreated material but nearly all coated materials as well. This may be a hint that a simple low temperature tempering of carbon-based materials in catalysts may suffice to have positive effects on ORR activity and hopefully immobilization of the noble metal catalyst with regard to long-term stability and durability. A similar phenomenon has been reported in the literature for activity towards the ORR[23] and electrical

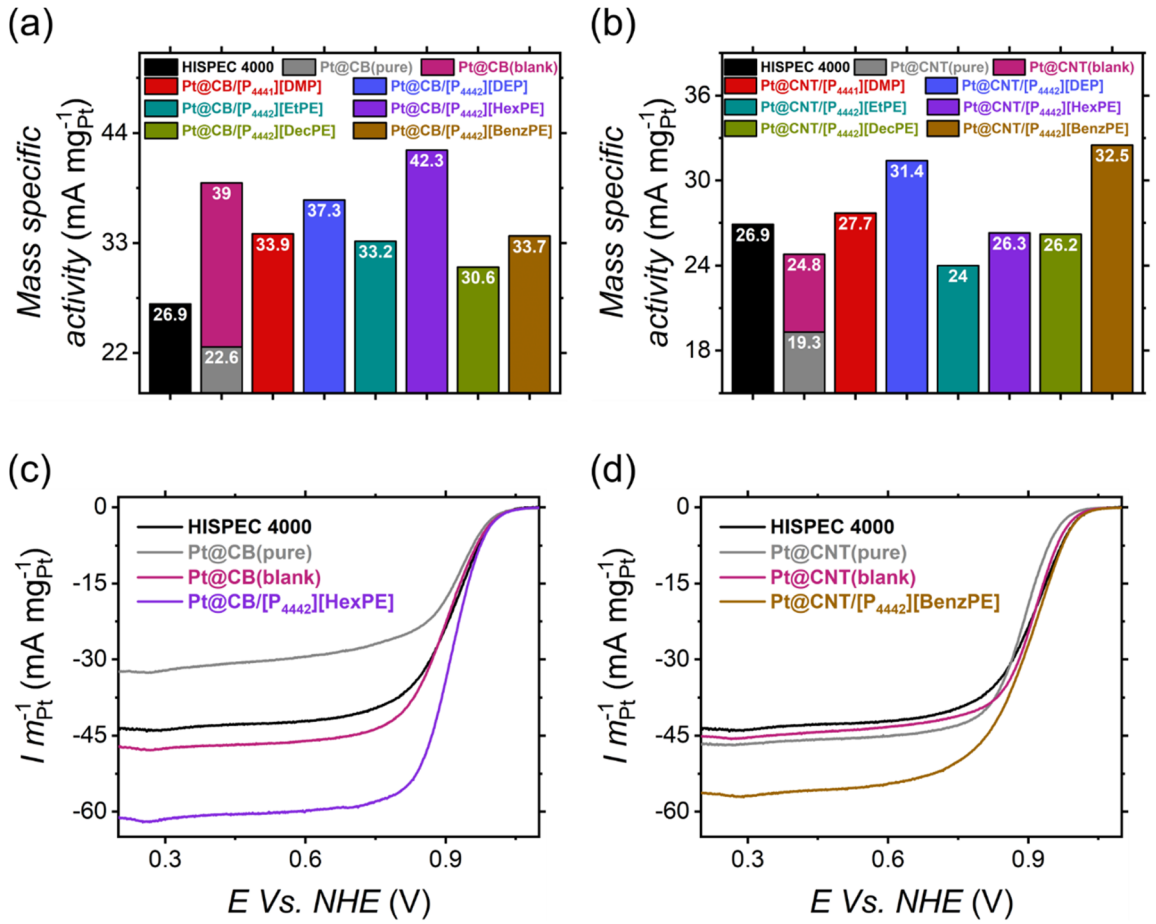

Fig. 1 Results of half-cell measurement of platinum deposited on pure and P-coated carbon materials in 0.1 M $HClO_4$. Mass specific activity of carbon black (a) and carbon nanotubes (b). Current per mass of platinum for carbon black (c) and carbon nanotubes (d). HISPEC® 4000 (platinum standard, nominally 40 wt% Pt@C) and the blank sample in comparison.

conductivity[24] due to graphitization at high temperatures. Regarding the method used in our investigations and stated earlier, a temperature treatment at 1000 °C was proven to decrease the ORR activity for catalysts from both P-coated carbon black and carbon nanotubes. A simple low temperature treatment with formation of phosphorus groups on the substrate surface prior to catalyst preparation seems to be remarkably more efficient in terms of mass specific activity towards the ORR, specifically for carbon nanotube catalysts.

Liu *et al.*[25,26] also investigated carbon nanotubes and found that Pt-decorated P- and P,N-doped CNTs possess increased stability in comparison to Pt-CNTs based on CV measurements. The authors suggested a higher binding energy for Pt bound to surface P and P,N and thus increasing the catalyst stability. Zhu *et al.* observed a similar trend when P was introduced in N-doped CNTs. The loss of mass activity for the P,N-CNTs was 19.3% after 5000 cycles in ADT, where the activity loss for N-CNTs was 50%. The authors suggested that P,N-doping favours the electron transfer to Pt, lowering the energy barrier for O_2 adsorption. Other literature[22,27–33] studies report similar observations, where P- or P,N-doping carbons showed increased activity and stability compared to heteroatom-free or single-doped carbons. The advantage of the presented approach is not limited to single-doping. With ionic liquids, co-doping of P,N may be achievable. Half-cell measurements of Pt_xP_y/C materials showed increased activity and stability in several literature reports.[34–37] Phosphorus in the Pt catalyst has a remarkable effect on ORR activity, presumably due to complete incorporation of P in the catalyst lattice without forming new phases. Lattice disorder in concave active sites decreases the binding energy of Pt–OH species, resulting in increased ORR activity.

A closer look at the two most promising combinations, Pt@CB/[P_{4442}][HexPE] and Pt@CNT/[P_{4442}][BenzPE] (designations [tri-butyl-ethyl-phosphonium][hexyl phosphonic acid ethyl ester] and [tri-butyl-ethyl-phosphonium][benzyl phosphonic acid ethyl ester], respectively), revealed that phosphorus coating has not only an impact on mass specific activity towards the ORR but also increases the current during ORR processing. Fig. 1c and d display the measured currents relative to the amount of platinum on the electrode of HISPEC® 4000, untreated, blank and the respective P-coated materials. The data reveal that the platinum mass-specific currents of P-coated materials exceed those of the HISPEC® 4000 platinum standard. P-coating increased the mass-specific current of untreated carbon black by almost 90%. For carbon nanotubes the effect is

less pronounced, yet significant as the current was increased by nearly 30%. A comparison between blank samples and P-coated materials shows that catalysts with heteroatom-containing carbons are superior to catalysts with pure carbon materials. Despite high mass specific activities of Pt@CB(blank) samples, they show only 66% of the current provided by Pt@CB/[P_{4442}][HexPE] during the ORR process. For CNT materials, the correlation of mass specific activity and current relative to the platinum mass shows a more linear behaviour. This phenomenon is in good agreement with other approaches reported in the literature, where P-containing carbon exhibited excellent characteristics for the ORR application.[22,38] Half-cell measurements reveal that P-coating of carbon black and carbon nanotubes increases both the ORR activity and current output. Lu and co-workers[21] made similar observations for their samples, where P was incorporated near the surface of the platinum layer. Both specific and mass activity were increased. In a similar fashion, P on the carbon surface may promote beneficial active sites for platinum nanoparticles.

The most promising P-coated materials were shown to be Pt@CB/[P_{4442}][HexPE] and Pt@CNT/[P_{4442}][BenzPE]. The platinum-decorated combinations were further characterized by means of electrochemical (Koutecky–Levich-plot), electronic (TEM) and structural (XRD) examinations as well as elemental (EDX), electronic (SEM) and structural (XPS) investigations for the pure materials. The Koutecky–Levich-plots of platinum-decorated samples with and without P-coating are shown in Fig. S7‡ with the respective average number of electrons $\bar{n}$. It can be seen that all four samples show a four-electron-mechanism for the oxygen reduction reaction as expected for the platinum-decorated catalysts.[39,40] The sample Pt@CB(pure) shows a non-linear plot, which can be attributed to a relatively poor RDE measurement. As can be seen in Fig. S8,‡ the current densities for Pt@CB(pure) measured for the rotational speed above 100 rpm are significantly lower than those for the sample Pt@CB/[P_{4442}][HexPE]. Therefore, the obtained plot should be interpreted with caution. Nonetheless, all platinum-decorated materials promote an ORR desirable 4-electron-mechanism.

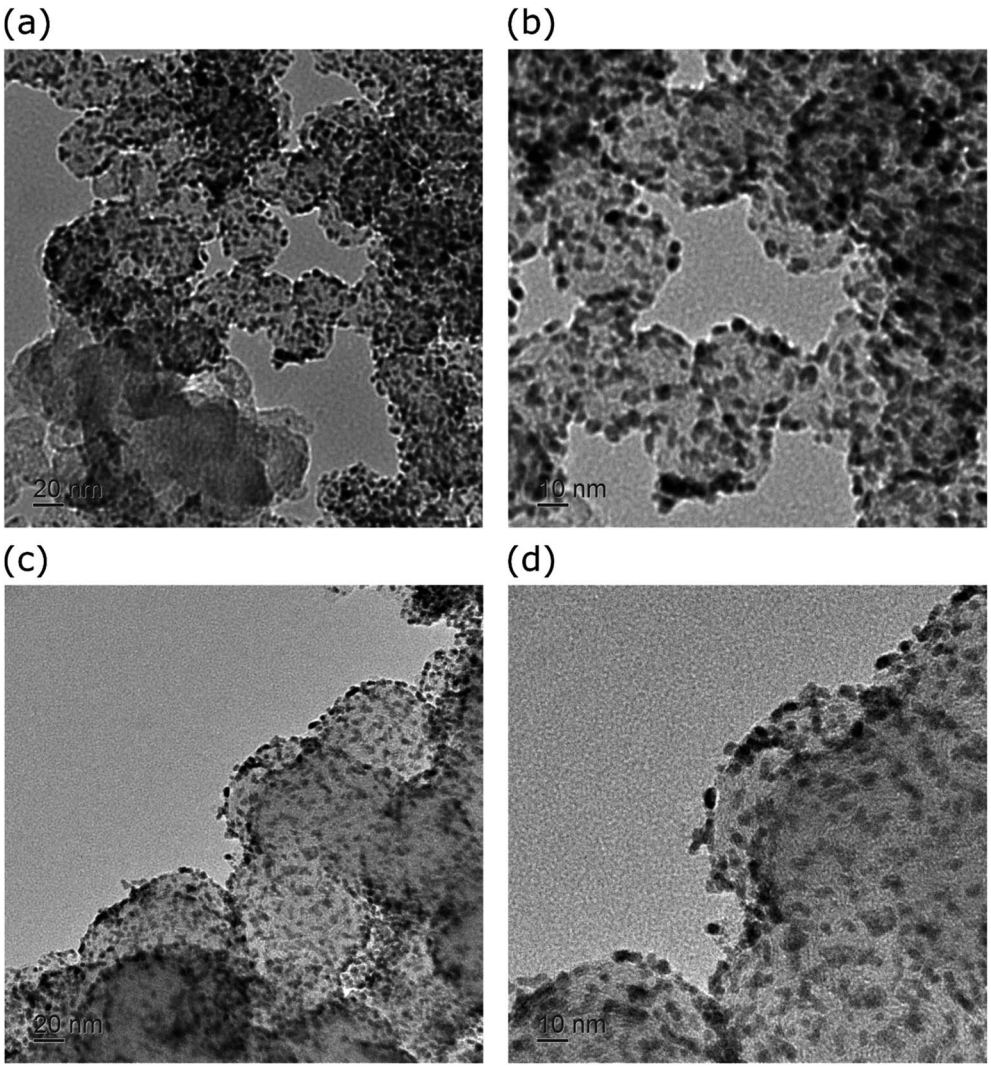

Fig. 2 TEM-images of the CB-based materials; (a) and (b) represent Pt@CB(pure) and (c) and (d) represent Pt@CB/[P_{4442}][HexPE].

To further investigate if P-coating affects the particle size and distribution of the decorated platinum nanoparticles, TEM-and XRD-measurements were carried out. TEM-images are shown in Fig. 2 and 3 and can be used to estimate the distribution of platinum nanoparticles on the material. As shown in the figures, platinum is evenly distributed for both CB samples without forming cluster regions. It can be concluded that Pt@CB/[P_{4442}][HexPE] shows a slightly more homogeneous distribution than Pt@CB(pure), with the latter possessing a blank area in the bottom middle region of Fig. 2a. The results may indicate for CB-based materials that P-coating prior to the deposition of the noble metal catalyst leads to a more homogeneous distribution and slightly smaller noble metal particles. A homogeneous distribution of platinum nanoparticles was also achieved by Willinger *et al.*[41] who studied the platinum–carbon interface of different carbons. As shown in Fig. 3, for the CNT-based materials no significant blank spaces are observed for the P-free samples, indicating evenly distributed nanoparticles. In contrast, the sample Pt@CNT/[P_{4442}][BenzPE] shows a significant number of areas without nanoparticles. The majority of platinum particles are heterogeneously distributed, and small clusters have been formed, identified by the large dark regions in the knots and threads of the nanotubes. In the studies of Liu *et al.*[25,26] the platinum nanoparticles decorated on P-doped CNTs were homogeneously distributed and showed no significant clusters. This difference between the CB- and CNT-based materials may be attributed to the difference in their morphology and surface area nature. CB consists of micro-sized spherical carbons with a surface area (BET) of around 240 m^2 g^{-1}, whereas CNTs are micro-scale threads with a BET surface area of around 67 m^2 g^{-1}. The applied method of platinum deposition by chemical reduction may henceforth be more suitable for CB-based materials than for CNT-based samples. Nonetheless, there are similar approaches for the chemical modification of carbon black[42,43] and carbon nanotubes,[44,45] as already described in the literature.

Lastly, platinum-decorated carbon materials were analysed by powder X-ray diffraction (XRD). The corresponding values

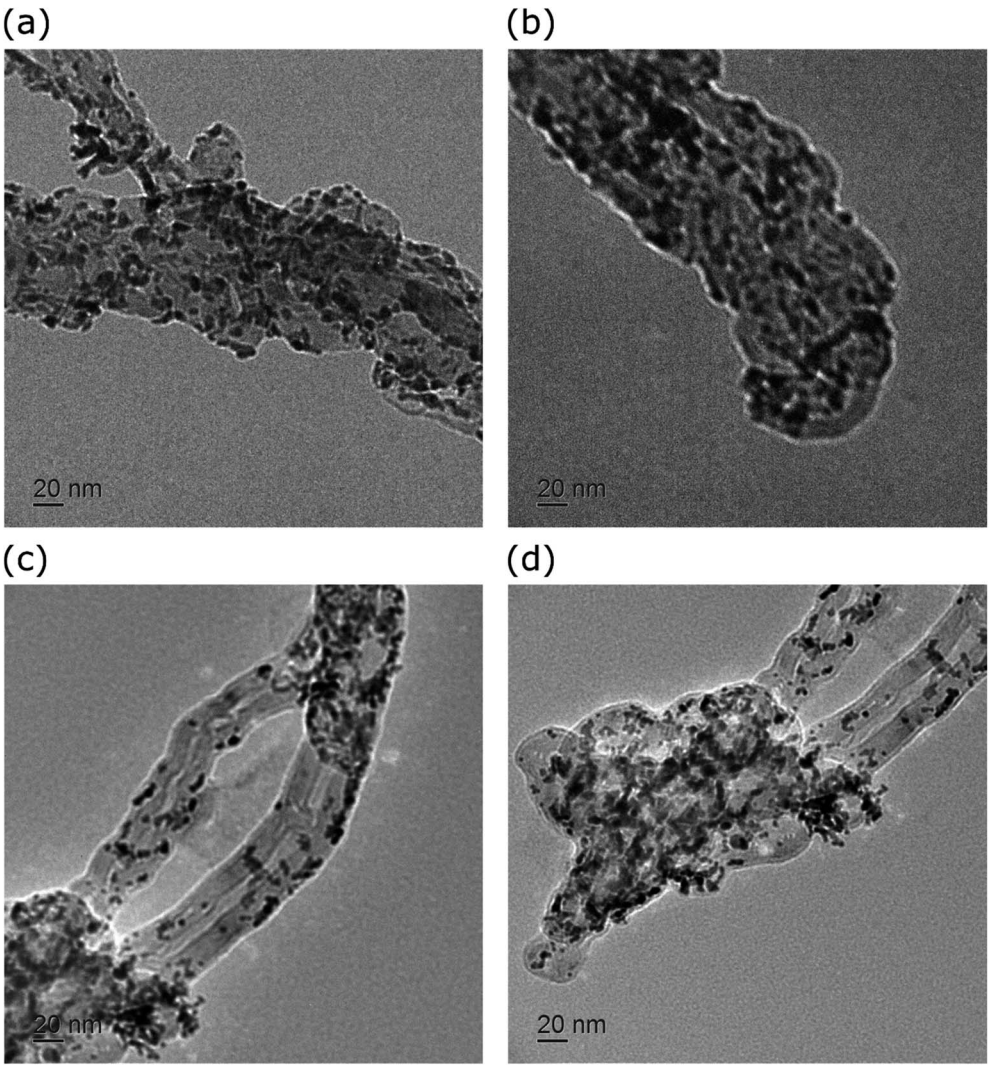

Fig. 3 TEM-images of the CB-based materials; (a) and (b) represent Pt@CNT(pure) and (c) and (d) represent Pt@CNT/[P_{4442}][BenzPE].

Table 1 Results of the Rietveld-refinement of platinum-decorated CB and CNTs; platinum row Pt shows the results corresponding to the platinum nanoparticles, and carbon row C-2H shows the results for the carbon phase; L_{vol} is the crystallite size, ω the weight-%, and a and c are the crystallite sizes along the a- and c-axes, respectively

Phase	Parameter	Pt@ CB(Pure)	Pt@ CNT(Pure)	Pt@CB/[P_{4442}][HexPE]	Pt@CNT/[P_{4442}][BenzPE]
Pt	L_{vol} (nm)	2.2	2.6	2.1	2.7
	ω (wt%)	51.4	53.0	48.6	54.7
	a (Å)	3.93	3.92	3.93	3.92
C-2H	L_{vol} (nm)	1.0	5.5	0.9	5.5
	ω (wt%)	48.6	47.0	51.4	46.3
	c (Å)	7.2	6.84	7.17	6.84

obtained from the analysis for platinum-phase Pt and carbon-phase C-2H are presented in Table 1. First, the given values for the weight-% ω should be treated with caution due to a high uncertainty. The general errors concerning stacking probability are estimated to be 5%. The uncertainty of the platinum loading can be assigned to the uncertain classification of the carbon phase, resulting in a difficult quantification of the platinum phase. Additionally, the quantification is hindered due to different adsorption coefficients of both phases. Therefore, the measured values from XRD are much higher in comparison to the ones obtained by TGA, see Table S1.‡ The (002)-reflex of the carbon phase is the most dominant factor influencing the a-axis (abbreviation a in Table 1) in the platinum phase. The results indicate that the CB-based materials have a much broader line width than the CNT-based samples. A crystallite size of 0.9 nm is remarkably similar to amorphous graphene and equals approximately the size of three graphite layers. The crystallite sizes of the CNT-based materials for both the platinum and carbon phases are slightly smaller than those for the CB-based samples. Similarly, the CNT-samples show a significant elongation along the c-axis (abbreviation c in Table 1) in comparison to the value of 6.71 nm found in the literature,[46] which can be attributed to the nature of the modification of the carbon nanotubes itself. The carbon nanotubes are not considered as typical graphite and may contain residual elements like nickel from their synthesis procedure. The deposited platinum is, after reviewing all results, nanocrystalline. The Rietveld-refinement showed that platinum is in a Cu-type fcc, in agreement with the literature.[38,47]

Fig. 4 shows SEM images with the corresponding elemental maps of carbon and phosphorus of synthesized PCC materials. The coating procedure did not alter the macroscopic morphology of the carbon substrate as it has been investigated during the initial stages of process optimization. The results associated with CB/[P_{4442}][HexPE] are displayed in Fig. 4a–c, and phosphorus is mainly evenly distributed with the exception of minor local clustering. The overall P-content in the sample was 1.4 wt% and 2.5 wt% in the cluster region. Fig. 4d–f show the results for CNT/[P_{4442}][BenzPE], where phosphorus is very evenly distributed without any cluster formation. The overall P-content according to EDX-measurement was about 2.6 wt%. The

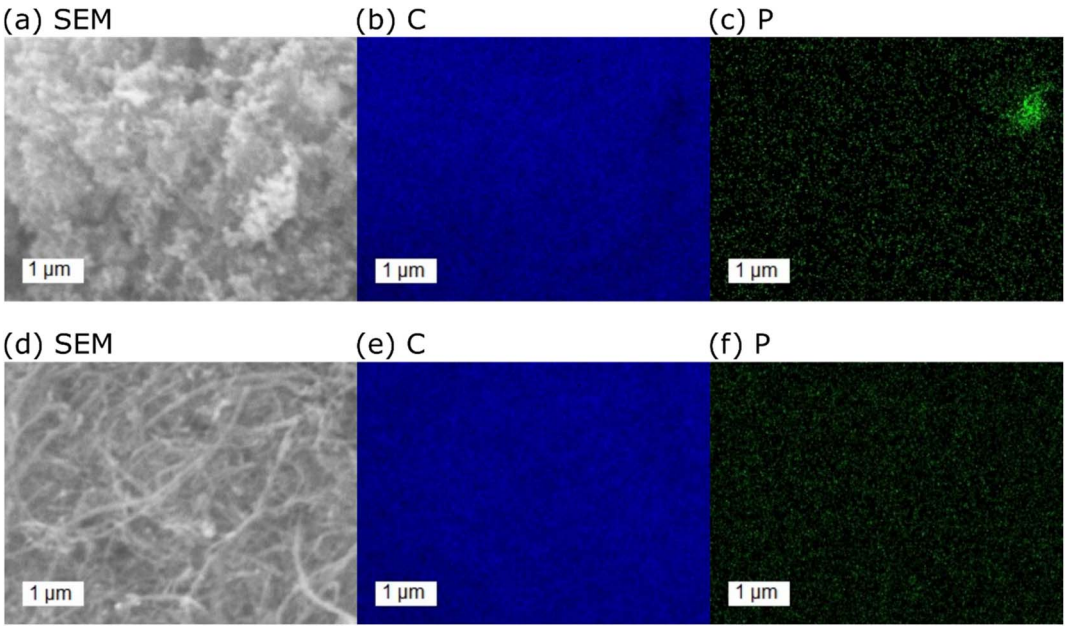

Fig. 4 SEM-image with the corresponding EDX-maps of CB/[P_{4442}][HexPE] (a)–(c) and CNT/[P_{4442}][BenzPE] (d)–(f). Blue dots in (b) and (e) represent the spots of carbon and green dots in (c) and (f) represent phosphorus detection.

Table 2 Powder conductivity of pure and P-coated carbon materials

	ρ (g cm^{-3})	σ (S cm^{-1})	σ increase by PCC coating (%)	P-content (EDX) (wt%)
CB pure	0.48	3.82	—	—
CB/[P_{4442}][HexPE]	0.54	4.30	+12.6	1.4
CNT pure	0.42	9.56	—	—
CNT/[P_{4442}][BenzPE]	0.51	9.68	+1.3	2.6

presence of phosphorus on the surface of carbon materials confirms the successful coating of different carbon materials with the usage of P-containing ionic liquids.

The investigation of conductivity is important for future application in fuel cells or other electronic devices. Table 2 gives an overview of the results for some of the carbon materials, where density, conductivity, increase in conductivity by phosphorus groups and P-content are displayed. The results show that phosphorus coating may increase the electrical conductivity depending on the tested carbon substrate. P-coating of carbon black-based materials leads to an increase of conductivity by 12.6% with an overall phosphorus content of 1.4 wt%. The effect of phosphorus is significantly lower for P-coated carbon nanotubes, where only 1.3% increase in conductivity is observed with an overall P-content of *ca.* 2.6 wt%. This may be due to the 2.5 times higher conductivity of untreated carbon nanotubes compared to that of untreated carbon black. This observation leads to the assumption that the positive effect of phosphorus coating on conductivity may be linked to the conductivity of the carbon substrate. The higher the conductivity of the untreated material, the lower the effect of P-coating on the conductivity. Different carbon substrates of both low and high conductivity could be investigated to assess this hypothesis. Nonetheless, a positive effect of P-coating on the conductivity can be observed within this work. In contrast to nitrogen, where positive charges at indirect neighbouring carbons (in the form of P–O–C bond formation in the presented work) are induced, phosphorus doping induces the active site on the phosphorus atom itself.[2] This results from the lower electronegativity of phosphorus compared to carbon; since phosphorus acts as an electron donor, the phosphorus atom will be positively charged.

In order to investigate the surface chemistry of P-coated carbon materials, XPS spectroscopy was used, as shown in Fig. 5. The P-2p XPS spectra shown in Fig. 5 were fitted by two 2p doublets. As constraints, the intensity ratio of the $2p_{3/2}$ and the $2p_{1/2}$ contributions of each doublet was set to 2 : 1 and the spin orbit splitting was fixed at 0.87 eV (ref. 48) which is close to the value of 0.84 eV, as given in Moulder's standard handbook.[49] As can be seen, phosphorus doping was successful for all samples, and phosphorus is present in two different species: PO_3^- and PO_4^- like. None of the other known phosphorus binding species with the other atoms present, such as C–P or P–P were detectable.[50] The binding energies for the investigated materials are listed in Table 4 and are in good agreement with data reported in the literature.[51] For P-coated carbon black, the two most promising combinations in terms of ORR-activity were investigated and the XPS results are displayed in Fig. 5a and b. For CB/[P_{4442}][DEP] (designation [tri-butyl-ethyl-phosphonium][diethyl-phosphate]), the majority (95%) of phosphorus is PO_4^- like bound and the minority (5%) of phosphorus is PO_3^- like bound. The binding characteristics of CB/[P_{4442}][HexPE] are in pronounced contrast to these results. In this sample, the majority (64%) of phosphorus is PO_3^- like bound, whereas the minority (36%) of phosphorus is PO_4^- like. The results for P-coated carbon nanotubes, represented in Fig. 5c and d, are more consistent. Both CNT/[P_{4442}][DEP] and CNT/[P_{4442}][BenzPE] possess almost only PO_4^- like P-binding, with only 1% or 2% of PO_3^- like phosphorus. The ratio of PO_3^- and PO_4^- like species in the samples may be traced back to the nature of the anion in the IL. For [P_{4442}][DEP] with a phosphate anion the results are as expected. The same is found for [P_{4442}][HexPE] where a phosphonate anion leads to mainly PO_3^- species. The exception is the IL [P_{4442}][BenzPE] which promotes the formation of PO_4^- species only, supposedly due to the reactive benzoyl structure in the anion. Table 3 shows the element content from XPS-measurements in at%. The oxygen to phosphorus atomic ratio from Table 3 is in accordance with the ratios of PO_3^-/PO_4^- like species and confirms that CB/[P_{4442}][HexPE] provides the highest P-content. This trend in phosphorus content is in good agreement with the TGA results presented in Fig. S8 and Table S5,‡ where [P_{4442}][DEP] showed the highest degree of residue-free decomposition per formula unit. With regard to the C1s spectra (see the ESI‡) we suggest the formation of C–O–P and P–O–P bridges between respective elements. Based on the C1s spectra, we propose that C–O–P-bridges make up the majority of P–O-species in the material. However, without data referring to the acidic nature of the carbon material a valid statement on P–OH-groups is not possible. Nonetheless, the presence of acidic groups on the surface has to be considered and would be in agreement with the literature.[8–11] Isolated PO_3^- and PO_4^- groups are likely formed on the surface after pyrolysis, but connected PO_3^- and PO_4^- groups (*i.e.* P_2O_6-species) are also possible. The differences in the integrated area in the C1s spectra attributed to C–O or C–P groups and overall O-content are affected by the shake-up satellites of carbon corresponding to C–C-bonding[52–54] Further details on this matter are described in the ESI.‡

Characterization of the surface chemistry of these innovative approaches towards creating P-doped carbons is barely investigated. Nonetheless, already described synthesis of PCC materials by other methods may serve as comparison to this novel technique. For example, Larrude *et al.*[50] identified different bonding environments for phosphorus in the XPS

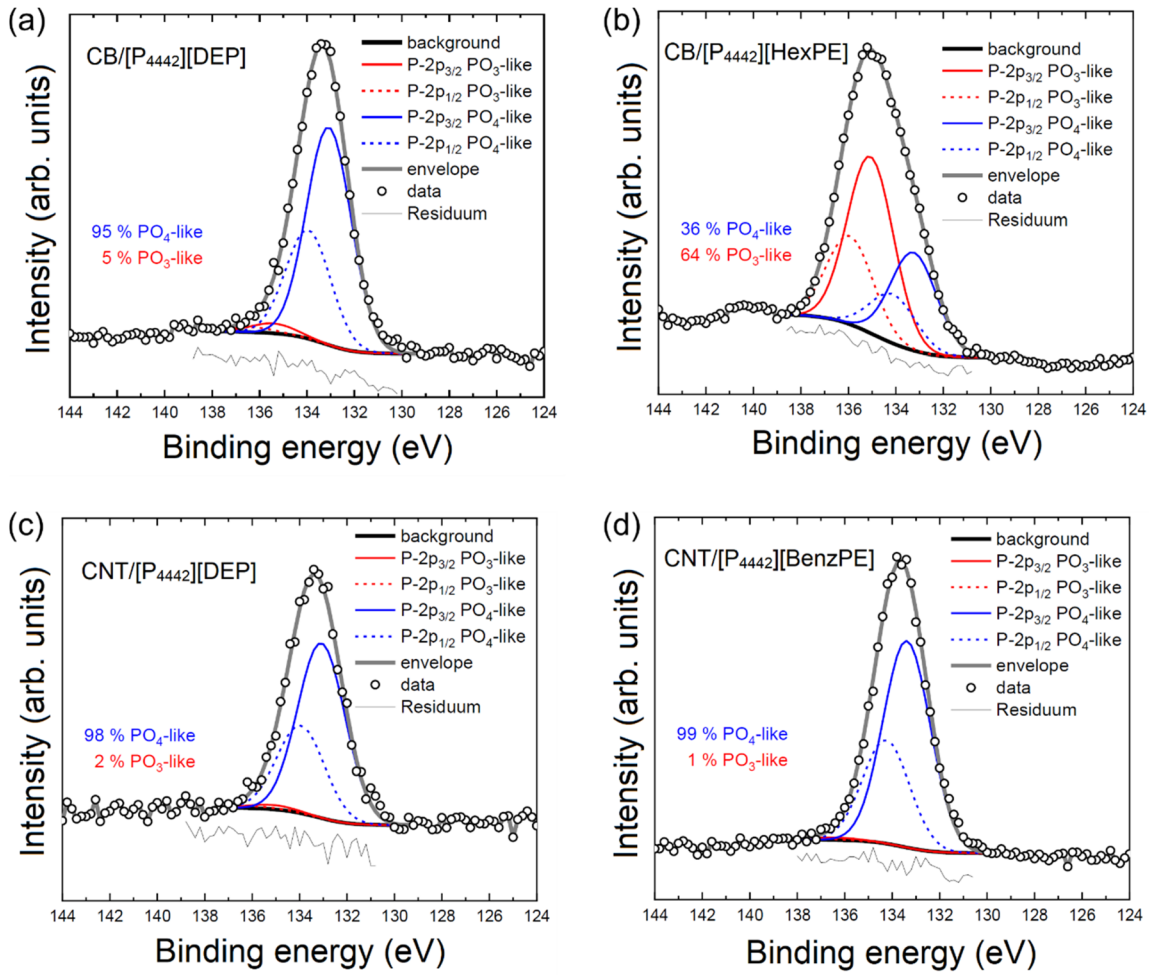

Fig. 5 Results from XPS-measurements of P-coated carbon black (a) and (b) and carbon nanotubes (c) and (d).

Table 3 Elemental composition of the samples (in terms of at%) as derived from XPS data

	C (at%)	O (at%)	P (at%)	Na (at%)
CB/[P_{4442}][DEP]	97.2	2.3	0.5	N.A.
CB/[P_{4442}][HexPE]	89.0	8.7	1.9	0.4
CNT/[P_{4442}][DEP]	97.4	2.2	0.4	N.A.
CNT/[P_{4442}][BenzPE]	94.2	4.6	1.2	N.A.

spectra and reported the respective chemical shifts. The working group synthesized phosphorus-doped carbon nanotubes with triphenylphosphine as the phosphorus source. Both C–P (129.5 eV) and P–O (133.3 eV) binding characteristics could be identified. The measurement of the XPS spectra of red phosphorus and triphenylphosphine served to distinguish between different bond formations of phosphorus. Differences between the phosphorus sources and the synthesized P-doped carbon nanotubes were easily discernible in the XPS-spectra. Rosas *et al.*[55] also reported chemical shifts of their P-doped carbon materials derived from lignin and phosphoric acid. The authors assigned the peaks to both C–PO_3 and C–O–PO_3 bonding environments, where the latter can be seen as PO_4^- like binding. The XPS data of Rosas and co-workers indicate mainly PO_3^- species in their P-containing carbon samples that were synthesized at 500 °C.[55] In a similar study, Liu *et al.*[56] synthesized P-doped activated carbon by impregnation with phosphoric acid and pyrolysis at different temperatures between 200 °C and 1000 °C. The results indicate that, with higher temperatures, the active phosphorus species switch from C–PO_3 and C_2–PO_2 to C–O–PO_3, with a maximum of C–O–PO_3 at 800 °C. The 800 °C sample provided the most promising electrocatalytical activity in half-cell measurements. Liu and co-workers stated that C–O–PO_3 species promote interfacial active sites that boost ORR activity.[56] This phenomenon may not be limited to half-cell-measurements but can also be applied for fuel cells, with C–O–PO_3^- or PO_4^- species being crucial for boosting performance. Li *et al.*[57] proposed that oxygen bridges in C–O–PO_3^- or PO_4^- species induce positive charges in the carbon matrix, promoting active sites and favouring O_2 adsorption. By weakening the O–O-bond of O_2, the reduction *via* 4-electron pathway of O_2 is then conducted. The results from all working groups are in good agreement with the obtained results and values displayed in Fig. 5 and Table 4. In this work, PO_3^- and PO_4^- like species in C–O–P setups are formed at noticeably

Table 4 Binding energies of P 2p signals of the samples as derived from XPS spectra

	Binding energy (eV)			
	PO_4^- like		PO_3^- like	
Carbon material	$2p_{3/2}$	$2p_{1/2}$	$2p_{3/2}$	$2p_{1/2}$
CB/[P_{4442}][DEP]	133.08	133.95	135.43	136.30
CB/[P_{4442}][HexPE]	133.25	134.12	135.06	135.93
CNT/[P_{4442}][DEP]	133.08	133.95	135.16	136.03
CNT/[P_{4442}][BenzPE]	133.38	134.25	136.38	137.25

lower temperatures when utilizing ionic liquids. A pyrolysis at 400 °C is sufficient to form the desired PO_4^- like-species, compared to the pyrolysis of phosphoric acid at 800 °C or 500 °C in the studies of Liu *et al.*[56] and Rosas *et al.*,[55] respectively. This shows the advancement of the presented approach in forming P-containing carbon layers on carbon materials. As an additional advantage, the method is not limited to specific carbon substrates with possibly a large variety of carbon materials being suitable for impregnation with ionic liquids. It is already reported in the literature[38] that PO_X-like species may have a beneficial impact on electro-catalytical properties. The most promising P-containing ordered mesoporous carbon exhibited a current density similar to a Pt/C catalyst (platinum standard, nominally 20 wt% Pt) and promoted a four-electron pathway for the oxygen reduction reaction. Additionally, it is reported that PO_X-like species are also formed in the Pt_xP_y catalyst, which are considered to have a remarkable effect on ORR activity.[34–37] It might be suggested that not only lattice distortion and the concave Pt-defects, but also PO_X bond formation may be beneficial for ORR activity and durability. Regarding the half-cell measurements conducted in this work, a similar trend for P-coated carbon materials can be observed.

5. Conclusions

Phosphorus doping of carbon materials proved to be crucial for boosting both durability and performance of electrochemical devices such as fuel cells. Phosphonium ionic liquids were utilized for coating of phosphorus species on carbon materials and were synthesized by a one-pot synthesis of tri-butylphosphine and a suitable anion precursor. Physicochemical characterization of both known and novel ionic liquids was performed (see the ESI‡) and revealed a high degree of ion aggregation. This observed phenomenon might be the reason for a lower polarity of the ionic liquids resulting in their good wetting behaviour observed in the nonpolar carbon materials. P-containing carbon materials were prepared by an adaptive wet impregnation method followed by pyrolysis at 400 °C. Half- and full-cell measurements confirmed the beneficial effect of phosphorus on the surface of carbon materials as catalyst supports for electrochemical applications like fuel cells with a four-electron ORR mechanism. Phosphorus-coating increased the mass activity towards the ORR and the current output in half-cell-measurements and improved the durability in fuel cell test systems compared to phosphorus-free materials and setups. The XRD and TEM measurements confirmed the homogeneous distribution of decorated platinum nanoparticles. Successful phosphorus deposition was demonstrated on both carbon black and carbon nanotubes with 1.4 wt% and 2.5 wt% phosphorus content, respectively. Furthermore, phosphorus-doping increased the electron conductivity by up to 12.6% for carbon black. The XPS-measurements revealed the formation of PO_3^- and PO_4^- like species on the substrate surface which are desirable for increasing ORR activity. The advantage of this study lies in formation of these phosphorus species at a relatively low pyrolysis temperature of 400 °C compared to previous studies. In conclusion, the presented novel approach of utilizing phosphonium ionic liquids as precursors for phosphorus group deposition *via* wet impregnation was proven to be suitable for the property modification of different carbon materials. These observations aid in enhancing the properties of carbon materials in diverse ways by a facile method and thus boosting the many applications in which C-materials are used. This covers in particular also the catalytic activity, performance, and durability of PEM-fuel cells by the improved carbon support.

Conflicts of interest

There are no conflicts to declare.

Acknowledgements

We acknowledge support by the Deutsche Forschungsgemeinschaft (DFG, German Research Foundation). We acknowledge the Industrial Research Community (IGF) for funding and enabling the research *via* the IGF-project no. 18 EWN. F. Müller and A. Holtsch acknowledge partial support from the German Research Foundation (DFG) *via* the Collaborative Research Center SFB 1027.

References

1 Z. Yang, J. Ren, Z. Zhang, X. Chen, G. Guan, L. Qiu, Y. Zhang and H. Peng, *Chem. Rev.*, 2015, **115**, 5159–5223.
2 D. Kim, O. Lun Li and N. Saito, *Phys. Chem. Chem. Phys.*, 2015, **17**, 407–413.
3 K. Mamtani and U. S. Ozkan, *Catal. Lett.*, 2015, **145**, 436–450.
4 Y. Sun, C. Li and G. Shi, *J. Mater. Chem.*, 2012, **22**, 12810–12816.
5 D. C. Higgins, D. Meza and Z. Chen, *J. Phys. Chem. C*, 2010, **114**, 21982–21988.
6 D. Yu, Q. Zhang and L. Dai, *J. Am. Chem. Soc.*, 2010, **132**, 15127–15129.
7 H. Jin, H. Zhang, H. Zhong and J. Zhang, *Energy Environ. Sci.*, 2011, **4**, 3389–3394.
8 D. W. McKee, C. L. Spiro and E. J. Lamby, *Carbon*, 1984, **22**, 285–290.
9 Y. Guo and D. A. Rockstraw, *Bioresour. Technol.*, 2007, **98**, 1513–1521.

10 P. F. Fulvio, R. T. Mayes, J. C. Bauer, X. Wang, S. M. Mahurin, G. M. Veith and S. Dai, *Catal. Today*, 2012, **186**, 12–19.
11 N. D. Lysenko, P. S. Yaremov, M. V. Ovcharova and V. G. Ilyin, *J. Mater. Sci.*, 2012, **47**, 3089–3095.
12 J. Bedia, J. M. Rosas, J. Rodríguez-Mirasol and T. Cordero, *Appl. Catal., B*, 2010, **94**, 8–18.
13 J. Laine, A. Calafat and M. Labady, *Carbon*, 1989, **27**, 191–195.
14 M. O. Guerrero-Pérez, J. M. Rosas, R. López-Medina, M. A. Bañares, J. Rodríguez-Mirasol and T. Cordero, *Catal. Commun.*, 2011, **12**, 989–992.
15 G. A. J. Amaratunga, V. S. Veerasamy, C. A. Davis, W. I. Milne, D. R. McKenzie, J. Yuan and M. Weiler, *J. Non-Cryst. Solids*, 1993, **164–166**, 1119–1122.
16 M. Rusop, S. M. Mominuzzaman, T. Soga, T. Jimbo and M. Umeno, *Jpn. J. Appl. Phys., Part 1*, 2003, **42**, 2339.
17 Y.-J. Lee and L. R. Radovic, *Carbon*, 2003, **41**, 1987–1997.
18 R. Imamura, K. Matsui, S. Takeda, J. Ozaki and A. Oya, *Carbon*, 1999, **37**, 261–267.
19 L. I. Şanlı, V. Bayram, B. Yarar, S. Ghobadi and S. A. Gürsel, *Int. J. Hydrogen Energy*, 2016, **41**, 3414–3427.
20 A. Egetenmeyer, I. Radev, D. Durneata, M. Baumgärtner, V. Peinecke, H. Natter and R. Hempelmann, *Int. J. Hydrogen Energy*, 2017, **42**, 13649–13660.
21 B.-A. Lu, L.-F. Shen, J. Liu, Q. Zhang, L.-Y. Wan, D. J. Morris, R.-X. Wang, Z.-Y. Zhou, G. Li, T. Sheng, L. Gu, P. Zhang, N. Tian and S.-G. Sun, *ACS Catal.*, 2021, **11**, 355–363.
22 J. Wu, C. Jin, Z. Yang, J. Tian and R. Yang, *Carbon*, 2015, **82**, 562–571.
23 W. Xia, J. Masa, M. Bron, W. Schuhmann and M. Muhler, *Electrochem. Commun.*, 2011, **13**, 593–596.
24 Yu. V. Surovikin, A. G. Shaitanov, I. V. Resanov and A. V. Syr'eva, *Procedia Eng.*, 2015, **113**, 519–524.
25 Z. Liu, Q. Shi, R. Zhang, Q. Wang, G. Kang and F. Peng, *J. Power Sources*, 2014, **268**, 171–175.
26 Z. Liu, J. Qu, X. Fu, Q. Wang, G. Zhong and F. Peng, *Mater. Lett.*, 2015, **142**, 115–118.
27 C. Deng, H. Zhong, X. Li, L. Yao and H. Zhang, *Nanoscale*, 2016, **8**, 1580–1587.
28 T. Najam, S. S. A. Shah, W. Ding, J. Jiang, L. Jia, W. Yao, L. Li and Z. Wei, *Angew. Chem., Int. Ed.*, 2018, **57**, 15101–15106.
29 C. H. Choi, S. H. Park and S. I. Woo, *ACS Nano*, 2012, **6**, 7084–7091.
30 N. Ranjbar Sahraie, J. P. Paraknowitsch, C. Göbel, A. Thomas and P. Strasser, *J. Am. Chem. Soc.*, 2014, **136**, 14486–14497.
31 R. Ma, B. Y. Xia, Y. Zhou, P. Li, Y. Chen, Q. Liu and J. Wang, *Carbon*, 2016, **102**, 58–65.
32 W. Ni, S. Liu, C. Du, Y. Fei, Y. He, X. Ma, L. Lu and Y. Deng, *Int. J. Hydrogen Energy*, 2017, **42**, 19019–19027.
33 J. Gao, C. He, J. Liu, P. Ren, H. Lu, J. Feng, Z. Zou, Z. Yin, X. Wen and X. Tan, *Catal. Sci. Technol.*, 2018, **8**, 1142–1150.
34 L. Zhang, M. Wei, S. Wang, Z. Li, L.-X. Ding and H. Wang, *Chem. Sci.*, 2015, **6**, 3211–3216.
35 R. Guo, W. Bi, K. Zhang, Y. Liu, C. Wang, Y. Zheng and M. Jin, *Chem. Mater.*, 2019, **31**, 8205–8211.
36 J. Ma, Y. Tang, G. Yang, Y. Chen, Q. Zhou, T. Lu and J. Zheng, *Appl. Surf. Sci.*, 2011, **257**, 6494–6497.
37 B.-A. Lu, L.-F. Shen, J. Liu, Q. Zhang, L.-Y. Wan, D. J. Morris, R.-X. Wang, Z.-Y. Zhou, G. Li, T. Sheng, L. Gu, P. Zhang, N. Tian and S.-G. Sun, *ACS Catal.*, 2021, **11**, 355–363.
38 D.-S. Yang, D. Bhattacharjya, S. Inamdar, J. Park and J.-S. Yu, *J. Am. Chem. Soc.*, 2012, **134**, 16127–16130.
39 M. Sakthivel, I. Radev, V. Peinecke and J.-F. Drillet, *J. Electrochem. Soc.*, 2015, **162**, F901–F906.
40 A. Bayrakçeken, A. Smirnova, U. Kitkamthorn, M. Aindow, L. Türker, İ. Eroğlu and C. Erkey, *J. Power Sources*, 2008, **179**, 532–540.
41 E. Willinger, A. Tarasov, R. Blume, A. Rinaldi, O. Timpe, C. Massué, M. Scherzer, J. Noack, R. Schlögl and M. G. Willinger, *ACS Catal.*, 2017, **7**, 4395–4407.
42 B. Fang, N. K. Chaudhari, M.-S. Kim, J. H. Kim and J.-S. Yu, *J. Am. Chem. Soc.*, 2009, **131**, 15330–15338.
43 Y. Kameya, T. Hayashi and M. Motosuke, *Appl. Catal., B*, 2016, **189**, 219–225.
44 R. Yu, L. Chen, Q. Liu, J. Lin, K.-L. Tan, S. C. Ng, H. S. O. Chan, G.-Q. Xu and T. S. A. Hor, *Chem. Mater.*, 1998, **10**, 718–722.
45 C. Xu, J. Chen, Y. Cui, Q. Han, H. Choo, P. K. Liaw and D. Wu, *Adv. Eng. Mater.*, 2006, **8**, 73–77.
46 P. Trucano and R. Chen, *Nature*, 1975, **258**, 136–137.
47 Z. Kaidanovych, Y. Kalishyn and P. Strizhak, *Adv. Nanopart.*, 2013, **02**, 32–38.
48 D. Chinnadurai, A. R. Selvaraj, R. Rajendiran, G. R. Kumar, H.-J. Kim, K. K. Viswanathan and K. Prabakar, *ACS Omega*, 2018, **3**, 1718–1725.
49 J. F. Moulder, W. F. Stickle, P. E. Sobol and K. D. Bomben, *Handbook of X-Ray Photoelectron Spectroscopy*, Perkin-Elmer Corporation, Eden Prairie, Minnisota, 1993.
50 D. G. Larrude, M. E. H. Maia da Costa, F. H. Monteiro, A. L. Pinto and F. L. Freire, *J. Appl. Phys.*, 2012, **111**, 064315.
51 A. M. Puziy, O. I. Poddubnaya, R. P. Socha, J. Gurgul and M. Wisniewski, *Carbon*, 2008, **46**, 2113–2123.
52 J. A. Leiro, M. H. Heinonen, T. Laiho and I. G. Batirev, *J. Electron Spectrosc. Relat. Phenom.*, 2003, **128**, 205–213.
53 B. Brena, Y. Luo, M. Nyberg, S. Carniato, K. Nilson, Y. Alfredsson, J. Åhlund, N. Mårtensson, H. Siegbahn and C. Puglia, *Phys. Rev. B: Condens. Matter Mater. Phys.*, 2004, **70**, 195214.
54 A. Majumdar, S. C. Das, T. Shripathi, J. Heinicke and R. Hippler, *Surf. Sci.*, 2013, **609**, 53–61.
55 J. M. Rosas, R. Ruiz-Rosas, J. Rodríguez-Mirasol and T. Cordero, *Carbon*, 2012, **50**, 1523–1537.
56 Y. Liu, K. Li, Y. Liu, L. Pu, Z. Chen and S. Deng, *J. Mater. Chem. A*, 2015, **3**, 21149–21158.
57 R. Li, Z. Wei, X. Gou and W. Xu, *RSC Adv.*, 2013, **3**, 9978–9984.

